

Extreme mass ratio inspiral rates: dependence on the massive black hole mass

Clovis Hopman

Leiden University, Leiden Observatory, P.O. Box 9513, NL-2300 RA Leiden

Abstract. We study the rate at which stars spiral into a massive black hole (MBH) due to the emission of gravitational waves (GWs), as a function of the mass M_\bullet of the MBH. In the context of our model, it is shown analytically that the rate approximately depends on the MBH mass as $M_\bullet^{-1/4}$. Numerical simulations confirm this result, and show that for all MBH masses, the event rate is highest for stellar black holes, followed by white dwarfs, and lowest for neutron stars. The Laser Interferometer Space Antenna (LISA) is expected to see hundreds of these extreme mass ratio inspirals per year. Since the event rate derived here formally diverges as $M_\bullet \rightarrow 0$, the model presented here cannot hold for MBHs of masses that are too low, and we discuss what the limitations of the model are.

PACS numbers: 98.62.Js, 02.70.Lq, 95.85.Sz, 98.10.+z, 97.60.-s

1. Introduction

The inspiral of a compact remnant into a massive black hole (MBH) leads to the emission of gravitational waves (GWs) with frequencies that will be detectable by the Laser Interferometer Space Antenna (LISA). Such extreme mass ratio inspirals (EMRIs) will lead to a wealth of astrophysical information, such as highly precise measurements of the mass and spin of the MBH, the mass of the inspiraling object, the distance to the source, and the direction of the source on the sky [7]. LISA will be sensitive to MBHs with masses in the range $10^4 M_\odot \lesssim M_\bullet \lesssim 10^7 M_\odot$, and is expected to detect thousands of events during its mission lifetime [14]. The existence of MBHs with masses $M_\bullet < 10^6 M_\odot$ is still hypothetical, in spite of considerable circumstantial evidence (see [37] for a review). Some of this evidence stems from ultra-luminous X-ray sources (ULXs). These are sources of X-rays that are more luminous than the Eddington luminosity for a $10 M_\odot$ stellar black hole (BH), but are located away from the center of their host galaxy, which makes it improbable that they are very massive, as dynamical friction would have brought them to the center. Arguments that selected ULXs are more massive than stellar BHs include mass estimates from the mass-temperature relation [35, 36] and quasi-periodic oscillations [10, 33]. Dynamical analysis also indicates that some globular clusters may contain quiescent intermediate mass BHs [19, 16, 39].

The rate at which EMRIs form near a given MBH is still rather uncertain, in part due to the scope of different dynamical processes that need to be taken into account. Estimates of event rates [23, 45, 38, 11, 32, 12, 2, 25, 26, 27] have typically focused on MBHs with masses

of $M_\bullet \sim 10^6 M_\odot$ (see [28] for a review). One reason for this is that the signal for such a MBH is strongest, but another, more practical reason, is that in that case the system can be scaled with the situation in the Galactic center, which contains a MBH of $M_\bullet \approx (3 - 4) \times 10^6 M_\odot$ [20, 44, 8, 21]. The Galactic center has been studied in great detail (see [1] for a review), and the knowledge we have of the stellar properties of the Galactic center can be exploited to calibrate models of stellar galactic nuclei.

A possible Ansatz to estimate event rates for lower mass MBHs is to assume that the empirical $M_\bullet - \sigma$ relation

$$M_\bullet = 10^8 M_\odot \left(\frac{\sigma}{200 \text{ km s}^{-1}} \right)^4 \quad (1)$$

between the M_\bullet and the velocity dispersion of the host galaxy [9, 17, 46] extends to lower mass MBHs. By making this assumption, inspiral rates for these hypothetical MBHs can be estimated. It should be stressed that the continuation of the $M_\bullet - \sigma$ relation to lower masses has no empirical foundation - indeed, the very existence of lower mass MBHs is not universally accepted.

One obvious interest in the detection of the inspiral into a lower mass MBH by LISA is that it would immediately provide unambiguous proof for the existence of such MBHs. In addition, an interesting possibility that is unique for lower mass MBH was suggested by [34, Sesana et al.(2008)Sesana, Vecchio, Eracleous, & Sigurdsson]. Since the tidal radius $r_t = (M_\bullet/M_\star)^{1/3} R_\star$ of a star with mass M_\star and radius R_\star has a weaker dependence on M_\bullet than the Schwarzschild radius $r_S = 2GM_\bullet/c^2$, tidal effects become more important compared to general relativistic effects as M_\bullet decreases. As a result, when MBHs of mass $M_\bullet \lesssim 10^5$ capture a white dwarf (WD), the WD may be disrupted by the tidal field during the last phases of inspiral. This may lead to a very interesting coincidence of a LISA detection with an electromagnetic counterpart. Lower mass MBHs also contribute differently to the stochastic background of GWs from EMRIs, due to the GWs emitted prior to the phase where they reach a signal to noise ratio high enough for detection [6].

These questions motivate us to revisit the dependence of the inspiral rate Γ on M_\bullet . [25] used analytical arguments to find $\Gamma \propto M_\bullet^{-1/4}$. Here we rephrase and extend these arguments for systems that include mass-segregation (§2). We then perform a series of numerical simulations, to derive the dependence $\Gamma(M_\bullet)$ numerically (§3), and show that the dependence is in good agreement with the analytical result. We discuss the validity, extensions, and consequences of our model in (§4).

2. EMRI rate model and scaling with mass

In order to compensate for our ignorance about lower mass MBH systems, we make the Ansatz discussed in the introduction of assuming that the $M_\bullet - \sigma$ relation can be extended to $M_\bullet < 10^6 M_\odot$, and we assume that the mass enclosed within the radius of influence $r_h = GM_\bullet/\sigma^2$ is proportional (and comparable) to that of the MBH. Based on these assumptions, we derive an analytical expression (12) for the dependence of the event rate on M_\bullet and present a numerical model to calculate these event rates.

2.1. Scaling galactic nuclei with mass

With the aforementioned assumptions, we find a number of scaling relations. The radius of influence, where the MBH dominates the potential, is given by

$$\begin{aligned} r_h &= \frac{GM_\bullet}{\sigma^2} \\ &= 2\text{pc} \left(\frac{M_\bullet}{3 \times 10^6 M_\odot} \right)^{1/2}. \end{aligned} \quad (2)$$

The fact that the enclosed mass of stars within r_h is proportional to the MBH mass implies that the number density at the radius depends on M_\bullet as

$$n_h = 4 \times 10^4 \text{pc}^{-3} \left(\frac{M_\bullet}{3 \times 10^6 M_\odot} \right)^{-1/2} \quad (3)$$

(for the normalization, see [18]).

The relaxation time then increases with the mass of the MBH as

$$\begin{aligned} T_h &= \frac{3(2\pi\sigma^2)^{3/2}}{32\pi^2 G^2 M_\star^2 n_h \ln \Lambda} \\ &= 6 \text{Gyr} \left(\frac{M_\bullet}{3 \times 10^6 M_\odot} \right)^{5/4}. \end{aligned} \quad (4)$$

In this expression, the Coulomb logarithm is approximately $\ln \Lambda = \ln(M_\bullet/M_\star)$; for our analytical arguments we discard the weak mass-dependence of the Coulomb logarithm.

2.2. Model for EMRI rate

We follow the analysis presented in [27], who solve the Fokker-Planck equations for a multi-mass model with 4 species: main sequence stars (MSs) of mass $M_{\text{MS}} = M_\odot$; WDs of mass $M_{\text{WD}} = 0.6M_\odot$; neutron stars (NSs) of mass $M_{\text{NS}} = 1.4M_\odot$; and stellar BHs of mass $M_{\text{BH}} = 10M_\odot$. In all cases we assume that the stars far away from the MBH have equal velocity dispersions σ , and that the unbound stars have a distribution function

$$g_M(x) = C_M \exp(x) \quad (x < 0), \quad (5)$$

where $x = E/\sigma^2$ is the dimensionless energy of the stars, and E is the negative specific energy with respect to the MBH. The prefactor C_M determines the fraction of compact remnants of type M in the unbound stellar population. The distribution (5) is what may be expected if the system was formed by violent relaxation; the stellar distribution of stars bound to the MBH is not very strongly affected by the exact form of this distribution (although it is dependent on its normalization), see e.g. [3]. To simplify our analysis, we do not consider the evolution of unbound stars, and assume that they are in steady state. This is mainly a simplification, but there is some justification in the fact that the relaxation time far away from the MBH

increases rapidly with distance, so that the dynamical evolution of these stars is slow. Also, there is likely star formation far away from the MBH, which will be harder to model, so that it is not clear how much realism would be obtained by including dynamics far away from the MBH. We note that the stellar models presented in [11, 13] do include dynamics for all stars in the system. For our models, we will assume that $C_M = (1, 0.1, 0.01, 0.001)$ for MSs, WDs, NSs and BHs, consistent with models of continuous star formation that appear to be consistent with Galactic center observations [4, 1].

The Fokker-Planck equations include a loss-cone term, and in dimensionless units, the equations have the following form (for details, see [27]; [3])

$$\frac{\partial g_M(x, \tau)}{\partial \tau} = -x^{5/2} \frac{\partial}{\partial x} Q_M - R_M(x), \quad (6)$$

where $R_M(x)$ is the rate at which stars of type M , with energies in the interval $(x, x + dx)$, reach the loss-cone and are eaten by the MBH. The rate at which stars flow through a given energy x is given by $Q = Q[g(x, \tau), x]$; this non-linear term represents 2-body relaxation. We stress that these equations do not depend on the MBH mass (apart from the assumption that it is much more massive than any of the individual stars). The same Fokker-Planck equation therefore applies to all systems, regardless of their MBH. The mass does enter, of course, in the dimension-full equations, and dictates for example how many years it takes to reach steady state.

The rate at which stars enter the loss-cone is much higher than the EMRI formation rate: many stars plunge prematurely without spiraling in. These stars never reach an orbit detectable by LISA.‡

In dimension-full units, the rate at which stars with semi-major axes less than a come into the loss-cone is then

$$\Gamma_M(< a) = 2\sqrt{2}I_0 \int_0^{a/r_h} dy y^{1/2} R_M(y), \quad (7)$$

where the flow I_0 is given by

$$\begin{aligned} I_0 &= \frac{8\pi^2}{3\sqrt{2}} r_h^3 n_h \frac{(GM_\star)^2 \ln \Lambda n_h}{\sigma^3} \\ &= 10^5 \text{ Gyr}^{-1} \left(\frac{M_\bullet}{3 \times 10^6 M_\odot} \right)^{-1/4}, \end{aligned} \quad (8)$$

which is approximately the number of the stars within r_h divided by the relaxation time. The actual flow is in some situations much smaller than I_0 (i.e., $\int_0^{a/r_h} dy y^{1/2} R_M(y) \ll 1$), as was realized by [5], who derived several analytical results from such “zero-flow” solutions. However, it was shown by [3] that in cases such as here, where there are very rare, massive objects (i.e., stellar BHs), maximal flows can in fact be achieved.

For LISA, the only objects that are accreted by the MBH and detected are those (compact) stars that spiral into the MBH gradually, without plunging prematurely into the

‡ An exception to this is the Galactic center where gravitational bursts from fly-bys are possibly detectable [43, 29, 47].

loss-cone. Therefore, for in-spirals, the integrand in equation (7) should be convolved with a function $S_M(a)$ that gives the probability for a star to spiral in without plunging. This function filters out all stars that plunge into the MBH without leading to a detectable EMRI source ("plunges"), and selects only the stars that do lead to a slowly inspiraling star. We compute this function with the Monte Carlo methods as described in [25] (see also [23], who used a very similar method). The total EMRI rate is then given by

$$\Gamma_M(< a) = 2\sqrt{2}I_0 \int_0^{a/r_h} dy y^{1/2} S_M(y) R_M(y). \quad (9)$$

The function $S_M(a/r_h)$ selects only those captured stars that spiral in successfully, which is a small fraction of the total number of captures [so $\int_0^{a/r_h} dy y^{1/2} S_M(y) R_M(y) \ll \int_0^{a/r_h} dy y^{1/2} R_M(y)$], of order 10% [2].

In contrast to the solution of the dimensionless Fokker-Planck equations, the function $S_M(a)$ may depend on the MBH mass, because the loss-cone, which is determined by the angular momentum of the last stable orbit $J_{\text{LSO}} = 4GM_\bullet/c$, depends on M_\bullet , and provide an additional length scale to the problem. However, it was argued by [25], that $S_M(a)$ can be approximated by a step-function that is zero for $a > a_c$, with

$$\frac{a_c}{r_h} = \left(\frac{d_c}{r_h} \right)^{3/(3-2p_M)}, \quad (10)$$

where

$$d_c \equiv \left(\frac{8\sqrt{GM_\bullet} E_1 T_h}{\pi c^2} \right)^{2/3}; \quad E_1 \equiv \frac{85\pi}{3 \times 2^{13}} \frac{M_\star c^2}{M_\bullet}, \quad (11)$$

and p_M is the slope of the distribution function $g_M(x)$. It follows that $d_c \propto M_\bullet^{1/2}$, and hence that a_c/r_h is independent of M_\bullet (see also figure 1). Hence, at the level of this approximation, it follows that the integral in equation (9) does not depend on mass, and thus that

$$\begin{aligned} \Gamma_M &= 2\sqrt{2}I_0 \int_0^\infty dy y^{1/2} S_M(y) R_M(y) \\ &\approx 2\sqrt{2}I_0 \int_0^{a_c/r_h} dy y^{1/2} R_M(y) \\ &\propto I_0 \propto M_\bullet^{-1/4}. \end{aligned} \quad (12)$$

The result (12) is derived from the assumption that $S_M(y)$ may be approximated by a step function $S_M(y) \approx \theta(a_c/r_h - y)$ with a_c/r_h as in equation (10). This result is based on several approximations compared to the numerical Fokker-Planck / Monte Carlo model. To test the validity of this approximate expression, we perform Monte Carlo experiments to determine the function S_M .

The calculation for the EMRI rate for all systems we consider here then goes through the following steps. (i) calculate the steady state of equations (6) once for all systems. (ii) From the outcome, find the dimensionless relaxation time

$$\tau_r(x) = \frac{M_\odot^2}{\sum_M g_M(x) M^2}. \quad (13)$$

(iii) Convert this dimensionless time-scale into a dimension-full time through equation (4), and use this time in the Monte Carlo simulations to find the function $S_M(a)$. (iv) Calculate the dimension-full integral (9) to calculate the EMRI rate.

3. Numerical results

We consider MBH masses of $M_\bullet = 3 \times 10^4 M_\odot$, $M_\bullet = 3 \times 10^5 M_\odot$, and $M_\bullet = 3 \times 10^6 M_\odot$, with stellar populations as indicated in §2.

In figure (1), we show the inspiral fractions $S_{\text{WD}}(a)$ for WDs for the MBH masses considered. Inspiral probabilities are high for small semi-major axes, as anticipated. The analytical arguments given in the previous section suggest that $S_{\text{WD}}(a/r_h)$ does not strongly depend on the MBH mass. To test this idea, we multiply the horizontal axis by $\sqrt{3 \times 10^6 M_\odot / M_\bullet}$ in order to extract the MBH dependence of r_h (equation 2). The curves now coincide approximately, confirming that the dependence on M_\bullet is weak. The figure also shows that $S_{\text{WD}}(a)$ can be reasonably approximated by a step-function.

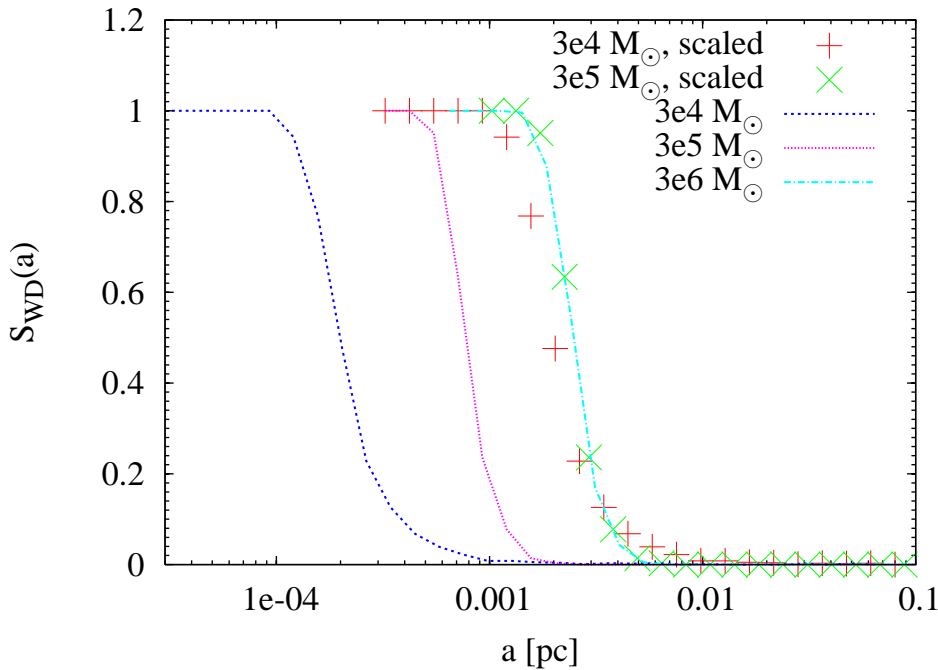


Figure 1. Inspiral fraction $S_{\text{WD}}(a)$ for WDs, for several MBH masses. The solid lines show the direct results, whereas the crossed data points were re-scaled by $\sqrt{3 \times 10^6 M_\odot / M_\bullet}$. The inspiral rate is high for small semi-major axes, and drops to zero at large semi-major axes, with $S_{\text{WD}} = 0.5$ at $\sim 2 \text{ mpc} (M_\bullet / 3 \times 10^6 M_\odot)^{-1/2}$. The fact that the scaled lines coincide with the line for $M_\bullet = 3 \times 10^6 M_\odot$ implies that $S_M(a/r_h)$ is to good approximation independent on the MBH mass.

The resulting event rates are reported for all different species in table (1). The numbers for $M_\bullet = 3 \times 10^6$ are different by a factor $\lesssim 2$ compared to those in [27], probably mainly due to slightly different boundary conditions.

Table 1. EMRI rates

M	WD	NS	BH
$[M_\odot]$	$[\text{Gyr}^{-1}]$	$[\text{Gyr}^{-1}]$	$[\text{Gyr}^{-1}]$
3×10^4	62	26	710
3×10^5	34	13	650
3×10^6	20	7	400

The event rates are plotted for the different species as a function of mass in figure (2). This figure shows that the event rate indeed decreases with M_\bullet , and the relation $\Gamma_M \propto M_\bullet^{-1/4}$ is confirmed.

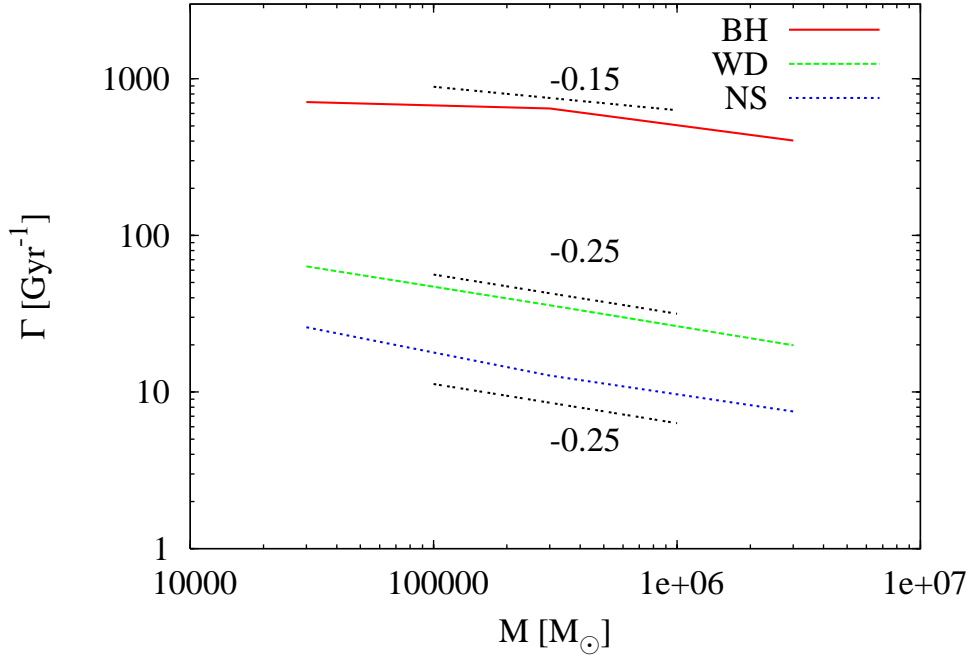


Figure 2. EMRI event rates as a function of MBH mass for BHs (top line), WDs (middle line), and NSs (bottom line). The straight lines give approximate power laws. For WDs and NSs the slope of -0.25 is in very good agreement with the analytical result, while for BHs, the slope of -0.15 is slightly flatter.

4. Summary and discussion

We analyzed the EMRI rate for several MBH masses in the context of the [25] and [27] models. The rate depends on MBH mass as $\Gamma_M \propto M_\bullet^{-1/4}$. The analytical mass dependence (equation 12) is confirmed by Monte Carlo simulations.

It is not trivial to calculate the projected EMRI detection rate from a given event rate [14]. The inspiral rate estimated here would give rise to a detection rate of $\sim 10^3$ over the

LISA life time of 5 years [15].

Since the event rate increases as the M_\bullet mass decreases, the assumptions for the models here must break down at some point, since otherwise the MBH would accrete more than its own mass within the age of the system. This is already the case for the $M_\bullet = 3 \times 10^4 M_\odot$ considered here. Several possible solutions to this paradox are that (i) such MBHs do not exist, or exist only during transient phases much shorter than the age of the Universe (for example, *because* of such high capture rates); or that (ii) somehow the assumed boundary conditions are not fulfilled, for example because the $M_\bullet - \sigma$ relation is not satisfied MBHs with $M_\bullet \lesssim 10^6 M_\odot$, or BHs do not sink in effectively from large distances, and are not formed by new star formation, so that the boundary condition for the unbound stars is not maintained over time. In the latter situation, the WD and NS rates, which are lower (and bring in less mass), could still be correct, and perhaps the actual rates would be even higher if stellar BHs do not push these stars out by mass segregation. To test this idea, we performed a simulation with a $M_\bullet = 3 \times 10^4 M_\odot$ MBH, similar to the ones presented in the previous sections, but without any stellar BHs. In this example, the event rate increases by a factor ~ 2.5 to $\Gamma_{\text{WD}} = 146 \text{Gyr}^{-1}$. We finally note that we find that the MBH grows as $M_\bullet \propto t^{4/5}$ as a result of EMRI captures, much slower than the exponential growth that would result from Eddington limited accretion.

In a recent paper, [40] study the stellar BH distribution around MBHs in a different context, where they consider cases with a much flatter mass function than we assume here, and with more massive stellar BHs. This will likely increase the EMRI rate further (and hence restrict further the MBH range for which the analysis is valid). Here we do not consider this situation.

The models presented here do *not* include the effects of resonant relaxation [42]. Resonant relaxation increases the rate at which the angular momenta of the stars randomize, but the effect is largely destroyed for very eccentric orbits due to general relativistic precession. It was argued by [26] that resonant relaxation will likely increase the EMRI rate by a factor of $\lesssim 10$. Many aspects of resonant relaxation remain unclear, however. Although the eccentricity dependence of random torques in a power-law cusp was found by [22], the coherence time of the torque, and its dependence on eccentricity, remain unknown. In addition, there is the related effect of resonant friction [42], which has not been considered so far in the literature in detail. It can be concluded that resonant relaxation will probably modify the EMRI event rate, but a more detailed analysis is premature at this point.

It has been suggested that triaxiality can also affect the EMRI rate [24]. Angular momentum is not a conserved quantity in a triaxial potential, and as a result it can potentially change much faster than can be achieved by relaxation mechanisms. However, it seems unlikely that the potential is significantly triaxial within the radius of influence, since the potential is there dominated by the MBH. Since $S_M(a) = 0$ for $a > 10^{-2} \text{pc}$ (see figure 1), enhanced evolution of angular momenta outside this distance would not lead to any additional EMRIs: if more stars are captured by the MBH, these captures will all result in plunges. Triaxiality outside the radius of influence can therefore only increase the capture rate of plunges. Similar conclusions apply to massive perturbers [41, 48].

We have focused on the direct capture of compact remnants by MBHs. An alternative route to making a LISA source with an intermediate mass black hole is by tidal capture of a main sequence star which circularizes near the MBH, and after it leaves the main sequence spirals into the MBH as a compact remnant [31, 30]. Such different formation mechanisms may lead to higher event rates.

Acknowledgments

I thank Alberto Lobo and Carlos Sopena for organizing a very fruitful LISA symposium. The work presented here was further developed at the 2W@AEI meeting at the Max-Planck Institut für Gravitationsphysik (Albert Einstein-Institut), organized by Pau Amaro-Seoane. I thank Jonathan Gair, Alberto Sesana and Pau Amaro-Seoane for encouraging me to investigate the mass dependence of EMRI rates in more detail, and Tal Alexander and Ann-Marie Madigan for comments on the manuscript. This work was supported by a Veni fellowship from the Netherlands Organization for Scientific Research (NWO).

References

- [1] Alexander, T. 2005, *Phys. Rep.*, 419, 65
- [2] Alexander, T., & Hopman, C. 2003, *Astrophys. J. Lett.*, 590, L29
- [3] —. 2008, ArXiv e-prints, (arXiv: 0808.3150)
- [4] Alexander, T., & Sternberg, A. 1999, *Astrophys. J.*, 520, 137
- [5] Bahcall, J. N., & Wolf, R. A. 1977, *Astrophys. J.*, 216, 883
- [6] Barack, L., & Cutler, C. 2004a, *Phys. Rev. D.*, 70, 122002
- [7] —. 2004b, *Phys. Rev. D.*, 69, 082005
- [8] Eisenhauer, F., et al. 2005, *Astrophys. J.*, 628, 246
- [9] Ferrarese, L., & Merritt, D. 2000, *Astrophys. J. Lett.*, 539, L9
- [10] Fiorito, R., & Titarchuk, L. 2004, *Astrophys. J. Lett.*, 614, L113
- [11] Freitag, M. 2001, *Classical and Quantum Gravity*, 18, 4033
- [12] —. 2003, *Astrophys. J. Lett.*, 583, L21
- [13] Freitag, M., Amaro-Seoane, P., & Kalogera, V. 2006, *Astrophys. J.*, 649, 91
- [14] Gair, J. R., Barack, L., Creighton, T., Cutler, C., Larson, S. L., Phinney, E. S., & Vallisneri, M. 2004, *Classical and Quantum Gravity*, 21, 1595
- [15] Gair, J. R. 2008, ArXiv e-prints (arXiv: 0811.0188)
- [16] Gebhardt, K., Rich, R. M., & Ho, L. C. 2005, *Astrophys. J.*, 634, 1093
- [17] Gebhardt, K., et al. 2000, *Astrophys. J. Lett.*, 539, L13
- [18] Genzel, R., et al. 2003, *Astrophys. J.*, 594, 812
- [19] Gerssen, J., van der Marel, R. P., Gebhardt, K., Guhathakurta, P., Peterson, R. C., & Pryor, C. 2002, *Astron. J.*, 124, 3270
- [20] Ghez, A. M., Klein, B. L., Morris, M., & Becklin, E. E. 1998, *Astrophys. J.*, 509, 678
- [21] Ghez, A. M., Salim, S., Weinberg, N., Lu, J., Do, T., Dunn, J. K., Matthews, K., Morris, M., Yelda, S., & Becklin, E. E. 2008, in *IAU Symposium*, Vol. 248, *IAU Symposium*, 52–58
- [22] Gürkan, M. A., & Hopman, C. 2007, *Mon. Not. R. Astron. Soc.*, 379, 1083
- [23] Hils, D., & Bender, P. L. 1995, *Astrophys. J. Lett.*, 445, L7
- [24] Holley-Bockelmann, K., & Sigurdsson, S. 2006, ArXiv: astro-ph/0601520
- [25] Hopman, C., & Alexander, T. 2005, *Astrophys. J.*, 629, 362
- [26] —. 2006a, *Astrophys. J.*, 645, 1152
- [27] —. 2006b, *Astrophys. J. Lett.*, 645, L133

- [28] Hopman, C. 2006, astro-ph/0608460, astro-ph/0608460
- [29] Hopman, C., Freitag, M., & Larson, S. L. 2007, *Mon. Not. R. Astron. Soc.*, 378, 129
- [30] Hopman, C., & Portegies Zwart, S. 2005, *Mon. Not. R. Astron. Soc.*, 363, L56
- [31] Hopman, C., Portegies Zwart, S. F., & Alexander, T. 2004, *Astrophys. J. Lett.*, 604, L101
- [32] Ivanov, P. B. 2002, *Mon. Not. R. Astron. Soc.*, 336, 373
- [33] Liu, J.-F., Bregman, J. N., Lloyd-Davies, E., Irwin, J., Espaillat, C., & Seitzer, P. 2005, *Astrophys. J. Lett.*, 621, L17
- [34] Menou, K., Haiman, Z., & Kocsis, B. 2008, *New Astronomy Review*, 51, 884
- [35] Miller, J. M., Fabbiano, G., Miller, M. C., & Fabian, A. C. 2003, *Astrophys. J. Lett.*, 585, L37
- [36] Miller, J. M., Fabian, A. C., & Miller, M. C. 2004, *Astrophys. J. Lett.*, 614, L117
- [37] Miller, M. C., & Colbert, E. J. M. 2004, *International Journal of Modern Physics D*, 13, 1
- [38] Miralda-Escudé, J., & Gould, A. 2000, *Astrophys. J.*, 545, 847
- [39] Noyola, E., Gebhardt, K., & Bergmann, M. 2008, *Astrophys. J.*, 676, 1008
- [40] O'Leary, R. M., Kocsis, B., & Loeb, A. 2008, ArXiv e-prints, (arXiv: 0807.2638)
- [41] Perets, H. B., Hopman, C., & Alexander, T. 2007, *Astrophys. J.*, 656, 709
- [42] Rauch, K. P., & Tremaine, S. 1996, *New Astronomy*, 1, 149
- [43] Rubbo, L. J., Holley-Bockelmann, K., & Finn, L. S. 2006, *Astrophys. J. Lett.*, 649, L25
- [44] Schödel, R., et al. 2002, *Nature*, 419, 694
- [Sesana et al.(2008)Sesana, Vecchio, Eracleous, & Sigurdsson] Sesana, A., Vecchio, A., Eracleous, M., & Sigurdsson, S. 2008, *Mon. Not. R. Astron. Soc.*, 391, 718
- [45] Sigurdsson, S., & Rees, M. J. 1997, *Mon. Not. R. Astron. Soc.*, 284, 318
- [46] Tremaine, S., et al. 2002, *Astrophys. J.*, 574, 740
- [47] Yunes, N., Sopuerta, C. F., Rubbo, L. J., & Holley-Bockelmann, K. 2008, *Astrophys. J.*, 675, 604
- [48] Zhang, M. 2009, ArXiv e-prints (arXiv: 0901.0301)